Volume 9, Issue 6, June – 2024 International Journal of Innovative Science and Research Technology
ISSN No:-2456-2165 https://doi.org/10.38124/ijisrt/IJISRT24JUN753

Geotechnical Assessment of Selected Lateritic Soils in Southwest Nigeria for Road Construction and Development of Artificial Neural Network Mathematical Based Model for Prediction of the California Bearing Ratio

Lateef Bankole Adamolekun[1*] · Muyideen Alade Saliu[1] · Abiodun Ismail Lawal[1] · Ismail Adeniyi Okewale[1]
[1]Department of Mining Engineering, School of Engineering and Engineering Technology,
Federal University of Technology, Akure, Nigeria

Corresponding Author: Lateef Bankole Adamolekun[1*]

Abstract:- Investigation of the geotechnical characteristics of eighteen different lateritic soils within southwest Nigeria was carried out to determine their suitability for road construction. To achieve this goal, the lateritic soils samples were subjected to different laboratory tests, including specific gravity, Atterberg limits, grain size analysis, California bearing ratio, and compaction, in accordance with the ASTM standard procedure. The results of the tests showed that the specific gravity varied between 2.55 and 2.81; the linear shrinkage varied between 6.68% and 10.98%; the liquid limit varied between 37.17% and 56.93%; the plastic limit ranged from 19.47% to 37.14%; the plasticity index ranged from 3.81% to 30.29%; the fine sand content ranged from 37.07% to 62..93%; the fines content ranged from 36.4% to 60.9%; the maximum dry density ranged from 1747 kg/m^3 to 2056 kg/m^3; the optimum moisture content ranges from 10.94% to 20.51%; the un-soaked California bearing ratio ranged from 14.7% to 45.6%; and the soaked California bearing ratio ranged from 10% to 31%. Based on these results, all the studied soils can be used as road subgrade, while none except Loc.5/S1 is suitable for road subbase. However, none of the soils meets up with the requirement for road base course. The suitability of laterite for the construction of road depends largely on the California bearing ratio. However, laboratory tests for determining the California bearing ratio is tedious, time consuming and costly. As a result of this difficulty, there is a need to develop soft computing models to predict laterite California bearing ratio from index properties with cheap and simple tests. Thus, the experimental datasets of the eighteen studied lateritic soils were used to create and train artificial neural network (ANN) models to predict California bearing ratio from liquid limits, plasticity index, linear shrinkage, fine sand content and fines content. The proposed ANN models were compared with the multiple linear regression models proposed in this study and various regression based models suggested in the literature via statistical analyses. Based on the model comparison, the proposed ANN models outperformed the rest of the models; they presented the highest R^2 and the lowest RMSE, MAPE and MAE values. Thus, the ANN models are validated. To enhance the practical application of the proposed ANN models, they were transformed into simple mathematical equations, which gave the same predictions as the direct ANN models. Thus, they can be used for practical purposes.

Keywords:- *Lateritic Soil, Geotechnical Property, Road Construction, Artificial Neural Network Model, California Bearing Ratio.*

I. INTRODUCTION

A road is a smooth surface over which a vehicle passes. It is built to connect places together, for easy convey of people and their properties. A road network is one of the key determinants of a country economic growth. Laterite is the most commonly used construction material in the tropics (Ayodele and Falade, 2016); most especially in road construction (Odunfa *et al.* 2018; Ogunribido and Fadairo, 2020; Owoyemi *et al.*, 2022, among others). Lateritic soil has distinct advantages as a road construction material, which includes its relative availability, low cost, and simple construction techniques. However, the alarming rate at which innocent lives are being lost due to the repeated failure of roads (Ogunribido and Fadairo, 2020; Owoyemi *et al.*, 2022 among others) calls for a solution. Studies (Ogundipe, 2008; Odunfa *et al.* 2018; Ogunribido and Fadairo, 2020 among others) revealed that some of the failures are caused by poor soil properties. A detailed examination of the geotechnical properties of lateritic soil before being used for road construction is needed to solve this problem. This seems to be lacking in our current day. The avoidance of laterite examination by some contractors can be attributed to high cost and time required to perform laboratory analyses of engineering properties most especially California bearing ratio. In this study, the

ISSN No:-2456-2165 https://doi.org/10.38124/ijisrt/IJISRT24JUN753

geotechnical properties of eighteen different lateritic soils within Southwestern Nigeria were assessed by subjecting their samples to different laboratory tests including specific gravity, linear shrinkage, Atterberg limits, grain size analysis, compaction and California bearing ratio, to determine their suitability for road construction, which is expected to assist contractors and field geotechnical engineers in quick selection of laterite for road construction. Furthermore, it is important to develop model to ease the determination of lateritic soils engineering properties such as California bearing ratio from index properties, which can be easily determined through simple and inexpensive tests (Khatti and Grover, 2021). Soft computing is an important branch of computational intelligence, where fuzzy logic, neural networks, and genetic algorithms are synergistically used to mimic the reasoning and decision making of a human (Lawal, 2020), and this include artificial neural networks (ANN), adaptive neural fuzzy inference systems (ANFISs), gene expression programming (GEP) and Gaussian process regression (GPR), among others. ANN is the most popular soft computing technique used by researchers (Lawal, 2020; Lawal and Idris, 2020; Lawal *et al*., 2021, among others). They have attracted greater interest for use in the prediction of soil properties (Tipza *et al*., 2014; Tenpe and Kaur, 2015 among others). However, the major drawback of most of the existing ANN models is that, their practical application is difficult for end users because they were not transformed into usable mathematical equations. Hence, this study developed ANN models to accurately predict California bearing ratio (soaked and unsoaked) from index properties, including liquid limits, plasticity index, linear shrinkage, fine sand content and fines content. To achieve this goal, the experimental dataset of the studied soils were used to create and train ANN models. The performance of the ANN models were compared with multiple linear regression (MLR) developed in this study and regression based models suggested in the literature. To enhance easy, accurate and quick prediction of the California bearing ratio (soaked and unsoaked), the proposed ANN models were transformed into simple mathematical models.

II. LITERATURE REVIEW

➢ *Laterite as a Road Construction Material*

Laterite can be used as subgrade, sub-base or base course of road (Jegede, 2004; Momoh *et al*., 2008; Ogundipe, 2008; Akintorinwa *et al.*, 2010; Onyelowe *et al.*, 2013; Nwankwoala *et al*., 2014; Amadi *et al*., 2015, among others). There are two main types of pavement: rigid and flexible. Rigid pavement is made with cement as the top layer, while flexible pavement is made with asphalt or bitumen as the top layer. In both rigid and flexible pavement, laterite is used as a subgrade. The strength of a material used as either a subbase or base course depends on its ability to transmit the axle load to the subsoil and/or subgrade (Amadi *et al*., 2015). However, one of the major causes of road accidents is bad roads, which are usually caused by the incorrect application of constructional materials, especially laterites, as sub-base and base course materials (Nwankwoala *et al*., 2014). Adequate information about the geotechnical properties of lateritic soil is essential for determining their suitability as road subgrade, subbase or base course, and this information include the particle size distribution, Atterberg limit, California bearing ratio (soaked and unsoaked), and compaction parameters.

The geotechnical property specifications for materiel recommended by the Nigeria Federal Ministry of Works and Housing, FMWH (1997), for road subgrade, subbase and base course material are as follows:

- The grain size distribution of subgrade or sub-base materiel must have fine content (percentage by weight passing through the No. 200 sieve) lesser than or equal to 35%;
- The Atterberg limits of subgrade material must have a liquid limit lesser than or equal to 50% and a plasticity index lesser than or equal to 20%, while subbase and base course material must have a liquid limit lesser than or equal to 35% and a plasticity index lesser than or equal to 12%;
- The maximum dry density and optimum moisture content of subgrade and subbase material should be greater than 1700 kg/m^3; and
- The unsoaked California bearing ratio of subgrade material must be greater than or equal to 10%, also, the subbase material must have a minimum soaked California bearing ratio of 30%, after at least 24 hours of soaking for heavy traffic, and the unsoaked California bearing ratio of base course material must be greater than or equal to 80%, while the soaked California bearing ratio must be at least 80% after at least 24 hours of soaking.

➢ *Description of Artificial Neural Network*

Artificial neural network (ANN) is a model inspired by the structure and function of biological neural networks in human brain; it process information just like human brain (Yang and Yang, 2014). ANN has the ability to learn and model non-linearity and complex relationships (Lawal *et al.* 2020). The artificial neural network architecture is determined by the number of layers, the number of nodes (neuron units) in each layer and the weighted connections between the nodes. The number of neurons in the hidden layer is determined by a trial-and-error process as there is no particular rule that govern this. ANN architectures can basically be classified into two categories, viz. feed-forward network and feedback or recurrent (Jain *et al*. 1996). The feed-forward network is a network in which the information in the model flows in only one direction, from the input nodes, through the hidden nodes and to the output nodes, without any cycles or loops nodes (Yang and Yang, 2014). Unlike feed-forward network, recurrent network has a bi-directional flow (Schmidhuber, 2015). Modern feed-forward network are using the back-propagation methods (Werbos, 1982, Lawal *et al*., 2020). The performance of each of the simulated ANN structure is evaluated using the coefficient of correlation (R) of the model predictions against the measured value and the ANN structure with the overall best performance (highest R value) is adopted.

ISSN No:-2456-2165 https://doi.org/10.38124/ijisrt/IJISRT24JUN753

III. EXPERIMENTAL INVESTIGATION AND MODELS DEVELOPMENT

➤ *Samples Collection and Laboratory Analyses*

Eighteen different laterite deposits within Southwest Nigeria were samples from Oyo, Ondo and Ekiti State, Southwest Nigeria. The samples were collected within the following coordinates: latitude 6°30'09.94" to 8°41'33.36" and longitude 3°26'13.34" to 5°44'44.72" (Fig. 1). Ten samples were randomly collected from each laterite deposit at a distance of 10 meters from each other within 1 m to 1.5 m depth. Approximately 15–20 kg of each sample was collected, put in nylon, sealed and taken to the laboratory for analysis. The obtained samples were subjected to various laboratory tests in accordance with ASTM standard procedure. The specific gravity of the samples was determined using a pycnometer (jar) according to the standard procedure of ASTM (2002) D 854-02.

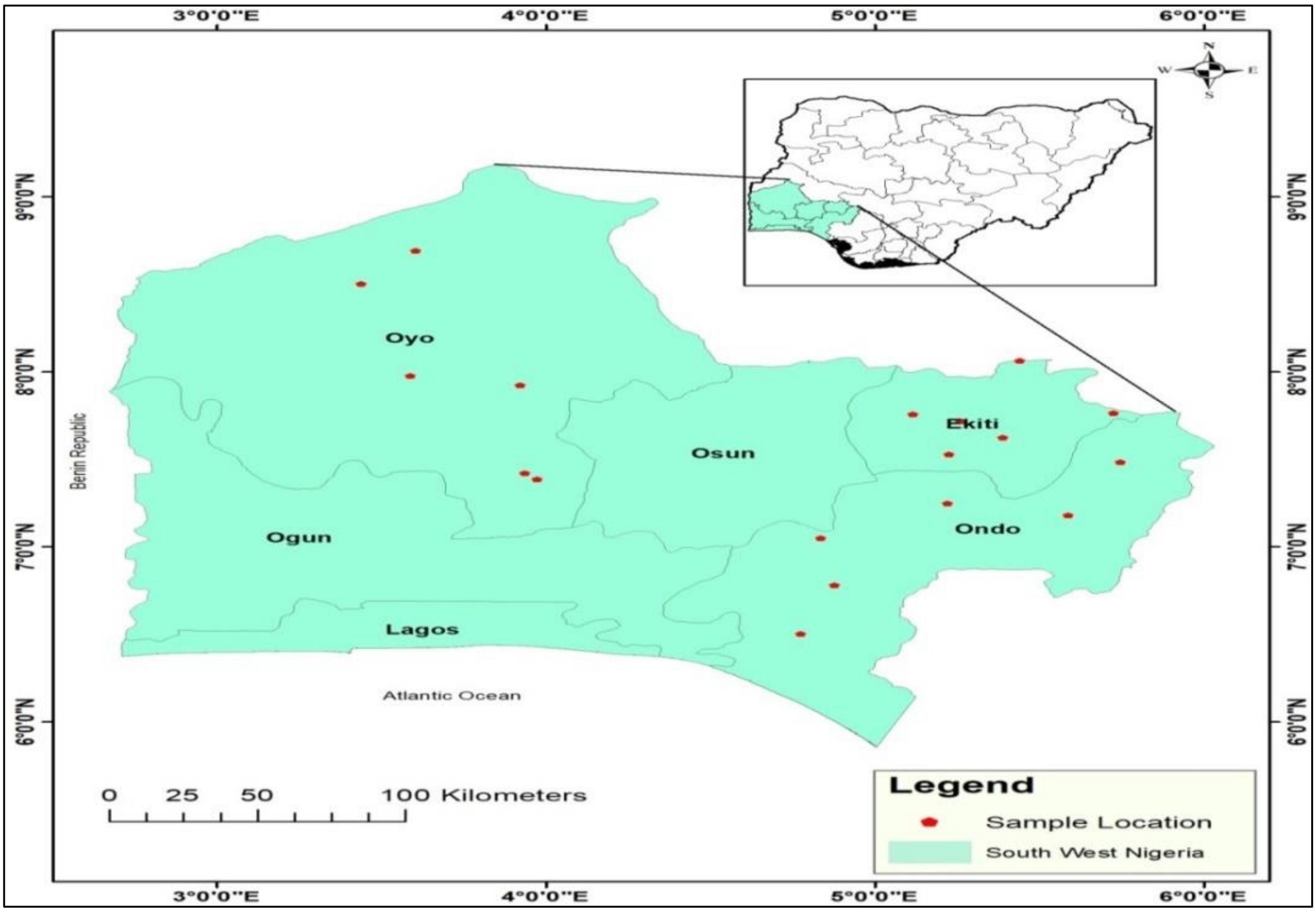

Fig 1 Map of Nigeria Showing the Sample Locations

Atterberg limit test was carried out on the samples in accordance with the standard procedure of ASTM (2018) D4318-17e1 to determine the plastic limit (PL) and liquid limit (LL). The plasticity index (PI) was estimated using Eq. (1).

$$PI = LL - PL \qquad (1)$$

The linear shrinkage of the samples was determined according to the standard procedure of ASTM (2002) D4943-02. A sieve analysis test was performed on the samples to determine the fine particle content. This test was carried out according to the standard procedure of ASTM (2002) D 422-63.

Table 1 Statistical Description of the Experimental Dataset

	SG	LL (%)	PL (%)	PI (%)	LS (%)	FC (%)	FSC (%)	MDD (kg/m^3)	OMC (%)	CBR_U (%)	CBR_S (%)
Mean	2.66	47.26	25.59	21.67	8.89	48.38	50.96	1892.74	15.68	29.26	19.90
Median	2.65	47.64	24.91	24.55	8.85	47.22	52.34	1892.05	15.79	29.28	19.91
StD	0.05	5.59	3.67	6.50	0.92	7.45	7.50	54.22	1.41	5.40	3.67
Min. val.	2.55	37.17	19.47	3.81	6.68	37.07	37.08	1789.75	11.89	19.83	13.49
Max. val.	2.81	56.93	37.14	30.29	10.98	60.92	62.93	2045.26	18.22	44.53	30.28
Kurtosis	-0.05	-1.26	1.87	-0.21	-0.49	-1.42	-1.34	0.58	0.20	0.28	0.28
Skewness	0.33	-0.15	1.54	-0.78	-0.08	0.006	-0.02	0.73	-0.67	0.53	0.53

ISSN No:-2456-2165 https://doi.org/10.38124/ijisrt/IJISRT24JUN753

StD standard deviation; Min. val. minimum value; Max. val. maximum value; SG specific gravity; LL liquid limit, %; PI plasticity index, %; LS linear shrinkage, %; FC percentage of passed $75\mu m$ sieve, %; FSC fine sand content, %; MDD maximum dry density, kg/m^3; OMC optimum moisture content, %; CBR_U unsoaked California bearing ratio, CBR_S soaked California bearing ratio, %.

The compaction test was conducted on the samples in accordance with the standard procedure of ASTM (2021) D698-12 to determine their maximum dry density and optimum moisture content. The California bearing ratio test was performed in accordance with the standard procedure of ASTM (2021) D1883-21. The statistical descriptions of the laboratory tests results are presented in Table 1. It can be deduced from Table 1 that the distributions of the geotechnical properties are largely close to normal as their Skewness are close to zero. Due to the large amount of data, the laboratory test results of the representative samples; first sample point from each location are presented in Table 2. The sample locations were labeled as Loc.1 to Loc.18. The acronyms S1 to S10 were used for the samples in each location.

Table 2 Geotechnical Properties of the Representative Samples

Sample Code	**SG**	**LL (%)**	**PL (%)**	**PI (%)**	**LS (%)**	**FSC (%)**	**FC (%)**	**MDD (kg/M^3)**	**OMC (%)**	**CBR_U (%)**	**CBR_S (%)**
Loc.1/S1	2.72	54.3	26.7	27.6	9.3	40.9	58.1	1855	17.38	25.5	17
Loc.2/S1	2.69	48.0	23.3	24.7	8.6	48.6	51.4	1925	15.36	32.5	22
Loc.3/S1	2.74	51.3	25.2	26.1	9.3	45.1	54.9	1889	16.42	28.9	20
Loc.4/S1	2.67	44.3	22.6	21.7	7.9	61.6	38.4	1966	14.18	38.0	26
Loc.5/S1	2.67	37.2	24.8	12.4	8.1	60.2	39.8	2045	11.89	44.5	30
Loc.6/S1	2.64	52.3	25.5	26.8	7.1	44.0	56.0	1878	16.74	27.8	19
Loc.7/S1	2.65	42.2	26.7	15.5	8.6	53.8	45.2	1901	15.19	30.1	20
Loc.8/S1	2.66	38.5	23.3	15.2	7.9	56.8	41.2	1949	13.86	34.9	24
Loc.9/S1	2.68	42.1	25.2	16.9	8.6	55.0	45.0	1902	15.16	30.2	21
Loc.10/S1	2.71	48.3	22.6	25.7	9.3	66.1	38.4	1891	15.46	38.0	26
Loc.11/S1	2.67	51.3	23.6	27.7	10.0	44.1	54.9	1856	16.42	34.0	23
Loc.12/S1	2.68	53.2	25.5	27.7	10.0	43.1	56.9	1833	17.02	23.3	16
Loc.13/S1	2.68	46.3	23.1	23.2	9.3	49.5	49.5	1847	16.67	24.7	17
Loc.14/S1	2.65	42.8	21.6	21.2	8.6	53.2	45.8	1893	15.41	29.3	20
Loc.15/S1	2.68	43.0	25.2	17.8	8.6	54.0	46.0	1890	15.48	29.0	20
Loc.16/S1	2.67	52.3	24.3	28.0	10.0	61.6	38.4	1844	16.74	24.4	17
Loc.17/S1	2.65	55.4	26	29.4	10.0	40.7	59.3	1808	17.73	20.8	14
Loc.18/S1	2.72	56.2	24.3	29.9	10.7	39.9	60.1	1798	17.98	19.8	13

SG specific gravity; LL liquid limit, %; PL plastic limit, %; PI plasticity index, %; LS linear shrinkage, %; FC percentage of passed $75\mu m$ sieve, %; FSC fine sand content, %; MDD maximum dry density, kg/m^3; OMC optimum moisture content, %; CBR_U un-soaked California bearing ratio, CBR_S soaked California bearing ratio, %.

The specific gravity (SG) of the studied soils ranged from 2.55 to 2.81. According to the FMWH (1997) specification, a good material for road construction should have specific gravity ranging from 2.5 to 2.75. Some of the soils have specific gravity values higher than 2.75, which made them unsuitable for road construction. The linear shrinkage (LS) of the studied soils ranged from 6.68% to 10.98%. Madedor (1983) recommended 8% maximum linear shrinkage for soil to be used as road subgrade. Based on this, only Loc.6/S1 and Loc.8/S1 conformed to the specification. The liquid limit (LL) of the studied soils ranged from 37.17% to 56.93%; the plastic limit (PL) ranged from 19.47% to 37.14%; and the plasticity index (PI) ranged from 3.81% to 30.29%. FMWH (1997) specified that for material to be used as road subgrade, its liquid limit must be lesser than or equal to 50% and plasticity index must be lesser than or equal to 20%. Also, for the case of subbase material, FMWH (1997) specified that the liquid limit must be lesser than or equal to 35% and plasticity index must be lesser than or equal to 12%. Based on this, all the studied soil can be used as subgrade, whereas only Loc.5/S1 conformed to the specification to be used as road subbase. The fine sand content (FSC) ranged from 37.07% to 62.93% and the fines content (FC) ranged from 36.4% and 60.9%. The maximum dry density (MDD) ranged from 1747 kg/m^3 to 2056 kg/m^3 and the optimum moisture content (OMC) ranged from 10.94% to 20.51%. FMWH (1997) specified that the maximum dry density of subgrade and subbase material should be 1700 kg/m^3 and above. All the soils have higher maximum dry density than 1700 kg/m^3, thus, they all conformed to the specification and can be used as road subgrade. The unsoaked California bearing ratio (CBR_U) ranged from 14.7% to 45.6%; and the soaked California bearing ratio (CBR_S) ranged from 10% to 31%. FMWH (1997) specified a minimum unsoaked CBR value of 10% for road subgrade; a minimum soaked CBR value of 30% for subbase; and at least 80% unsoaked and soaked CBR value for base course material. Based on this, all the soils meet the requirement to be used as road subgrade, whereas, only Loc.5/S1 conformed to the specification to be used as road subbase. In summary, the engineering application of the studied soils for road construction is presented in Table 3.

ISSN No:-2456-2165 https://doi.org/10.38124/ijisrt/IJISRT24JUN753

Table 3 Suitability of the Studies Laterite for Road Construction

Sample code	**Road sub-grade**	**Road sub-base**	**Road base**
Loc.1/S1	YES	NO	NO
Loc.2/S1	YES	NO	NO
Loc.3/S1	YES	NO	NO
Loc.4/S1	YES	NO	NO
Loc.5/S1	YES	YES	NO
Loc.6/S1	YES	NO	NO
Loc.7/S1	YES	NO	NO
Loc.8/S1	YES	NO	NO
Loc.9/S1	YES	NO	NO
Loc.10/S1	YES	NO	NO
Loc.11/S1	YES	NO	NO
Loc.12/S1	YES	NO	NO
Loc.13/S1	YES	NO	NO
Loc.14/S1	YES	NO	NO
Loc.15/S1	YES	NO	NO
Loc.16/S1	YES	NO	NO
Loc.17/S1	YES	NO	NO
Loc.18/S1	YES	NO	NO

As shown in Table 3, all the studied soils can be used as road subgrade, and Loc.5/S1 soil can be used as road subbase course.

- *Models Development*

Artificial neural network (ANN) and multiple linear regression (MLR) models were developed for the prediction of CBR_U, and CBR_S with costly and tedious laboratory test, from index properties with cheap and simple tests. This is expected to assist contractors and field engineer in quick assessment of laterite CBR_U, and CBR_S.

- *Variable Selection and Normalization*

A correlation matrix was carried out on the soil parameters using Pearson's correlation. A correlation matrix is a statistical technique used to evaluate the strength of the relationship between two variables in a dataset. It was used in this study to select independent variables (index properties) for the prediction of CBR_U and CBR_S using ANN and MLR models. The correlation matrix results are presented in Table 4. The correlation matrix showed that LS, LL, PI, FSC, and FC have high correlation values (ranged from 0.531 to 0.912) with CBR_U and CBR_S, than did the other index properties, SG and PL, with correlation values ranging from - 0.18 to 0.069. Thus, LS, LL, PI, FSC and FC were selected as the model predictors for CBR_U, and CBR_S predictive models.

Table 4 Correlation Matrix of the Dataset Variables

Variables	SG	LS	LL	PL	PI	FSC	FC	OMC	MDD	CBR_U	CBR_S
SG	**1**	0.338	0.091	-0.047	0.105	-0.079	0.080	-0.028	0.096	0.069	0.069
LS	0.338	**1**	0.637	0.038	0.527	-0.427	0.424	0.630	-0.694	-0.630	-0.630
LL	0.091	0.637	**1**	0.062	0.826	-0.727	0.731	0.903	-0.810	-0.735	-0.735
PL	-0.047	0.038	0.062	**1**	-0.511	-0.174	0.179	0.175	-0.171	-0.180	-0.180
PI	0.105	0.527	0.826	-0.511	**1**	-0.528	0.528	0.679	-0.601	-0.531	-0.531
FSC	-0.079	-0.427	-0.727	-0.174	-0.528	**1**	-0.993	-0.746	0.653	0.624	0.624
FC	0.080	0.424	0.731	0.179	0.528	-0.993	**1**	0.751	-0.655	-0.632	-0.632
OMC	-0.028	0.630	0.903	0.175	0.679	-0.746	0.751	**1**	-0.966	-0.888	-0.888
MDD	0.096	-0.694	-0.810	-0.171	-0.601	0.653	-0.655	-0.966	**1**	0.912	0.912
CBR_U	0.069	-0.630	-0.735	-0.180	-0.531	0.624	-0.632	-0.888	0.912	**1**	1.000
CBR_S	0.069	-0.630	-0.735	-0.180	-0.531	0.624	-0.632	-0.888	0.912	1.000	**1**

The proposed models are five-input, one-output models that were trained using a total of one hundred and eighty (180) experimental datasets. The input and output data for the ANN models were normalized between -1 and 1 using Eq. (2) to achieve dimensional consistency of the parameters and to eliminate over fitting of the trained network (Lawal 2020).

$$Y_i = \frac{(R_{max} - R_{min})(X_i - X_{min})}{X_{max} - X_{\min}} + R_{min} \quad (2)$$

Where Y_i is the normalized parameter, X_i is the actual data to be normalized, R_{max} is the maximum value of the range of normalization, R_{min} is the minimum value of the range of normalization, and X_{max} and X_{min} are the maximum and minimum values of the actual data, respectively.

- *Proposed Artificial Neural Network Model*

ANN was implemented in MATLAB software using a total of one hundred and eighty (180) datasets. The datasets were divided into training, testing and validation datasets (70% (126 dataset) for training and 15% (27 dataset) each for testing and validation) and loaded into the software to develop the models. The ANN models were developed in 5-N-1 architecture format (one input layer, one hidden layer and one output layer). The number of neurons in the hidden layer was determined by a trial-and-error process starting from 2 and increasing progressively at an interval of 1. A nonlinear tan sigmoid (TANSIG) and linear (PURLIN) transfer function was used for the hidden and output layers, respectively. The performances of each of the simulated ANN structures were evaluated using the coefficient of correlation (R) of the model predictions against the measured value. The optimum ANN structure with the overall best performance (highest R value) for training, validation, and testing datasets, was adopted for accurate prediction of CBR_U and CBR_S. In this study, the 5-8-1 architecture (Fig. 2) exhibited the overall best performance for CBR_U and CBR_S.

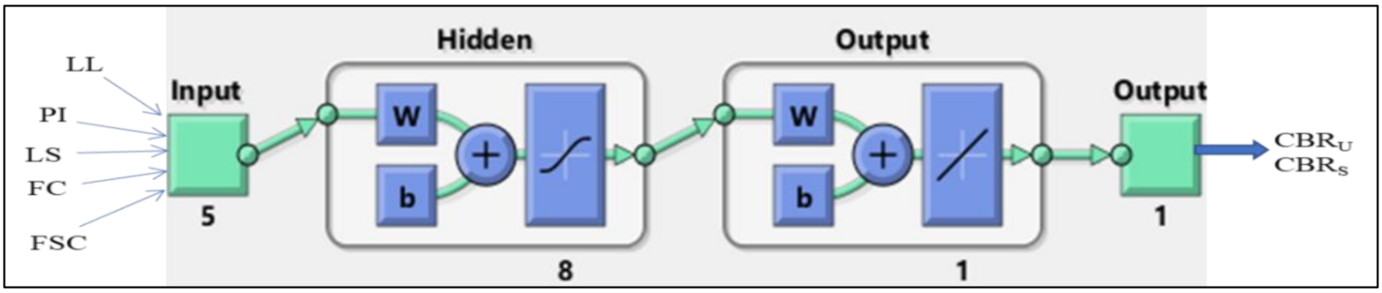

Fig 2 Proposed ANN Models Architecture for CBR_U and CBR_S

- *Multiple Linear Regression (MLR)*

MLR analysis was performed in Microsoft Excel software Add-ins using the same one hundred and eighty (180) datasets used in training the soft computing models. Linear regression was selected under the analysis drawdown, and both the dependent and independent variables were loaded into it to perform the required MLR analysis. The obtained multiple linear regression (MLR) equations for CBR_U and CBR_S are presented in Eqs. (3 and 4)

$$CBR_U = 103.05 - 0.54\ LL + 0.16\ PI - 1.69\ LS - 0.30\ FSC - 0.44\ FC \quad (3)$$

$$CBR_S = 70.08 - 0.37\ LL + 0.11\ PI - 1.15\ LS - 0.20\ FSC - 0.30\ FC \quad (4)$$

IV. RESULTS AND DISCUSSION

➢ *Proposed Models' Performances*

To validate the proposed ANN models, the models performances were compared with the MLR models developed in this study and the prominent regression based analysis suggested in the literature, listed in Table 5.

Table 5 Existing Empirical Models in the Literature for Predicting Permeability

S/N Existing Model	Reference	Eq./N
1. $CBR_U = 0.2930\ LL + 0.0663\ FC + 12.3209$	Torgano *et al*. (2020)	(5)
2. $CBR_U = 0.715\ LL + 2e^{-13}$	Adejumo and Tsado (2019)	(6)
3. $CBR_U = -0.3018\ FC + 50.132$	Owoseni *et al*. (2012)	(7)
4. $CBR_S = -0.1681\ FC + 26.02$	Torgano *et al*. (2020)	(8)
5. $CBR_S = -0.1\ LL - 0.425\ PI + 15.73$	Gudeta and Patel (2018)	(9)
6. $CBR_S = -0.221\ FC + 26.6$	Owoseni *et al*. (2012)	(10)

The models were made to predict the whole experimental dataset and their predictions were compared to the laboratory measured values, and their performances were assessed using the coefficient of determination (R^2), root mean squared error (RMSE), mean absolute percentage error (MAPE), and mean absolute error (MAE), as shown in Eqs. (11) to (15) and the results are presented in Table 6.

$$R^2 = 1 - \frac{\sum_{i=1}^{n}(E-P)^2}{\sum_{i=1}^{n}(E-\bar{Y})^2} \quad (11)$$

Where

$$\bar{Y} = \frac{1}{n}\sum_{i=1}^{n} E \quad (12)$$

$$RMSE = \sqrt{\frac{1}{n}\sum_{i=1}^{n}(E-P)^2} \quad (13)$$

$$MAPE = \frac{1}{n}\sum_{i=1}^{n}\frac{(E-P)}{E} \times 100 \quad (14)$$

$$MAE = \frac{1}{n}\sum_{i=1}^{n}|E - P| \quad (15)$$

Where n is the number of sample data points used for the model development, E and P represent the measured and predicted values of the CBR_U and CBR_S, respectively, and $\bar{Y}$ is the mean of the measured CBR_U and CBR_S.

Table 6 Performance Indices

Model	CBR_U				CBR_S			
	R^2	**RMSE**	**MAPE**	**MAE**	**R^2**	**RMSE**	**MAPE**	**MAE**
Proposed ANN	0.873	1.9234	5.1919	1.2197	0.870	1.745	1.2495	0.188
Proposed MLR	0.622	3.3147	8.4520	2.5026	0.622	2.257	8.5638	1.720
Torgan *et al*. (2020)	0.559	7.0250	20.419	5.7362	0.4	3.636	13.397	2.857
Adejumo and Tsado (2019)	0.540	9.8444	30.132	7.8992	-	-	-	-
Gudeta and Patel (2018)	-	-	-	-	0.336	18.384	92.504	18.107
Owoseni *et al*. (2012)	0.4	7.62	25.726	6.7540	0.4	4.9411	19.435	4.1612

For the prediction of CBR_U (Table 6), ANN model outperformed the MLR model proposed in this study and the regression based models in the literature suggested by Torgan *et al*. (2020), Adejumo and Tsado (2019) and Owoseni *et al*. (2012) by presenting the highest R^2 and the lowest RMSE, MAPE, and MAE values. ANN model presented R^2 value of 0.873, indicating that the input parameters explained over 87.3% of the variation in the measured CBR_U.

For the case of CBR_S (Table 6), ANN model presented the highest R^2 value compared to the MLR proposed in this study and the regression based models suggested by Torgan *et al*. (2020), Gudeta and Patel (2018) and Owoseni *et al*. (2012). ANN model presented R^2 value of 0.870, indicating that using the ANN model; the input parameters explained over 87% of the variation in the measured CBR_S. Furthermore, ANN model presented the lowest RMSE, MAPE and MAE values, indicating that it has low prediction error than did the MLR model proposed in this study and the regression based models suggested by Torgan *et al*. (2020), Gudeta and Patel (2018) and Owoseni *et al*. (2012) in the literature.

In summary, the ANN models proposed in this study performed better than the proposed MLR and regression based models suggested in the literature for the prediction of both CBR_U and CBR_S. Thus, the ANN models are validated and can be used for practical purposes.

- *Transformation of the ANN Models to Simple Mathematical Equations*

To enhance the practical application of the proposed ANN models, the models were transformed into simple mathematical equations based on the ANN general equation shown in Eq. (16).

$$y = f_{purlin}\{b_0 + \sum_{k=1}^{n}[f_{sig}(b_{bk} + \sum_{i=1}^{m} w_{ik}\, x_i) \times w_k]\} \quad (16)$$

Where is the bias in the output layer; is the weight of the connection between the of the hidden layer and the single output neuron; is the bias in the neuron of the hidden layer; m is the number of neurons in the input layer; n is the number of neurons in the hidden layer; is the weight of the connection between the input parameter and the hidden layer; is the input variable i; y is the output variable; and and are the transfer functions, which are linear and nonlinear transfer functions, respectively.

The mathematical equation obtained for the CBR_U and CBR_S are presented in Eqs. (17) and (18).

$$CBR_U = 12.35\text{purlin}\,(0.346138 - 0.13634\,x_1 + 0.695433\,x_2 - 3.2264\,x_3 - 2.38615\,x_4 - 1.31347\,x_5 + 1.033\,x_6 + 1.819086\,x_7 + 0.192862\,x_8) + 32.15 \quad (17)$$

Where

x_1 = tanh (-1.83364+ 0.766374 LS + 1.052102 LL – 0.91475 PI + 0.485579 FSC + 1.279949 FC)

x_2 = tanh (2.173298+ 2.856703 LS - 2.75082 LL + 0.136457 PI + 2.022581 FSC - 2.25912 FC)

x_3 = tanh (-0.12645 + 0.379016 LS - 0.62907 LL - 0.29342 PI + 0.914414 FSC + 0.686156 FC)

x_4 = tanh (4.504852 - 1.91097 LS + 3.77619 LL - 0.48593 PI - 0.17276 FSC + 1.189861 FC)

x_5 = tanh (0.397564+ 1.054611 LS - 0.98754 LL + 0.852154 PI - 2.65626 FSC - 1.82013 FC)

x_6 = tanh (-1.22093 + 1.811044 LS - 2.98728 LL - 0.0448 PI + 0.13451 FSC - 0.39653 FC)

x_7 = tanh (2.550866 + 1.449535 LS - 3.1406 LL + 0.099161 PI - 1.3004 FSC + 0.064673 FC)

x_8 = tanh (1.16893 + 3.131742 LS + 0.189647 LL + 0.739034 PI + 0.631931 FSC - 0.04899 FC)

$$CBR_S = 8.5\text{purlin}\,(0.210835 + 0.339058\,y_1 + 0.741802\,y_2 - 3.1708\,y_3 - 2.08764\,y_4 - 1.27721\,y_5 + 0.521102\,y_6 + 1.760423\,y_7 + 0.303801\,y_8) + 21.5 \quad (18)$$

Where

y_1 = tanh (-2.754 + 1.598783 LS + 0.32544 LL - 0.73961 PI - 0.50894 FSC + 0.821193 FC)

y_2 = tanh (2.022313 + 2.44397 LS - 2.57039 LL + 0.326427 PI + 2.182111 FSC - 1.61017 FC)

y_3 = tanh (0.226619 + 0.603693 LS - 0.70504 LL - 0.60867 PI + 0.795601 FSC + 0.718686 FC)

y_4 = tanh (1.468544 - 1.61509 LS + 2.845184 LL - 0.53763 PI + 0.543166 FSC - 0.08487 FC)

$$y_5 = \tanh(-0.07264 + 0.704068\ \text{LS} - 1.36563\ \text{LL} + 1.675483\ \text{PI} - 3.02601\ \text{FSC} - 1.90094\ \text{FC})$$

$$y_6 = \tanh(-0.94314 - 1.18641\ \text{LS} - 0.58044\ \text{LL} - 1.22753\ \text{PI} - 0.93102\ \text{FSC} - 0.25963\ \text{FC})$$

$$y_7 = \tanh(2.922779 + 1.569906\ \text{LS} - 3.04166 - 0.37728 - 1.97583\ \text{FSC} - 0.08998\ \text{FC})$$

$$y_8 = \tanh(1.701532 + 2.83055\ \text{LS} - 0.217\ \text{LL} - 0.14703\ \text{PI} + 0.62698\ \text{FSC} + 0.234794\ \text{FC})$$

➢ *Validation of the ANN Mathematical Models*

The predictions directly output from the ANN models and that of Eqs. (17 and 18) were compared using the whole datasets to validate the mathematically transformed ANN models. The comparison, as illustrated in Fig. 6, showed that the R^2 for both CBR_U and CBR_S model is 1, indicating that the mathematical equations explained 100% of the variation in the direct ANN model predictions. Hence, the equations are validated and can be used directly for predicting the CBR_U and CBR_S of lateritic soils in the studied area.

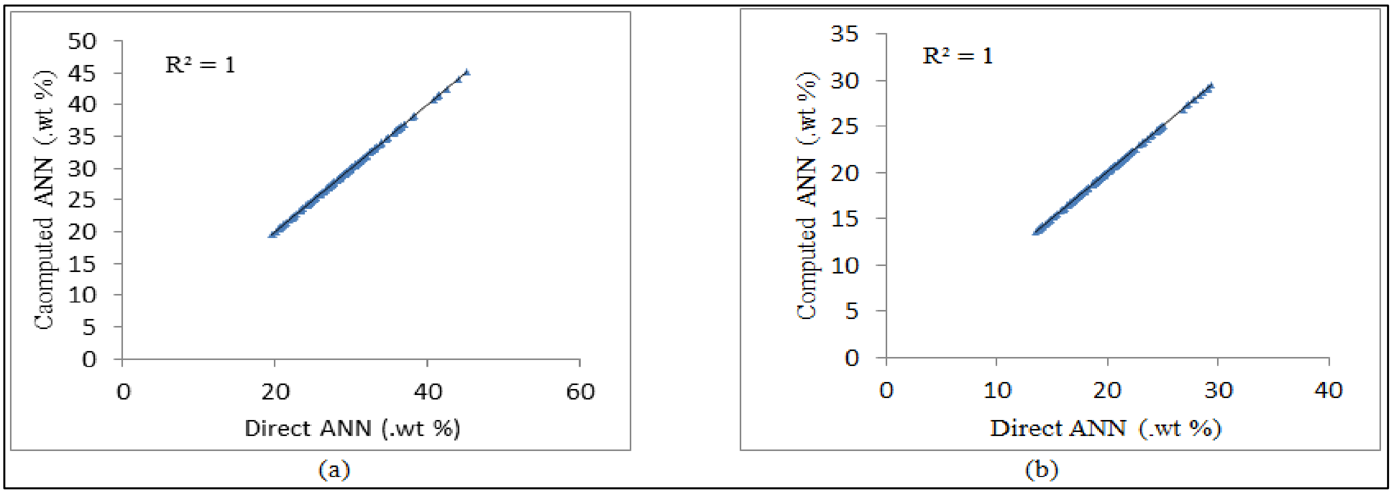

Fig 3 Comparison of the ANN Mathematical Model and Direct Simulated Output for (a) CBR_U (b) CBR_S

➢ *Sensitivity Analysis*

Sensitivity analysis is a technique used to evaluate the input parameter that most affects the output parameters. The cosine amplitude method (CAM) is one of the most reliable methods for evaluating the input parameters that most strongly affect the output parameters (Jong and Lee 2004). This was used in this study, as presented in Eq. (19), to identify the significance of each input parameter (LL, PI, LS, FC and FSC) on the outputs (CBR_U and CBR_S), predicted by the proposed ANN models.

$$R_{ij} = \frac{\sum_{k=1}^{n}(\text{I} \times \text{P})}{\sqrt{\sum_{k=1}^{n}\text{I}^2 \sum_{i=1}^{n}\text{P}^2}} \tag{19}$$

Where R_{ij} represents the strength of the input parameter, I represents the model input, P is the predicted output, and n is the number of data points. The significance of each of the input parameters on the ANN models predictions are presented in Fig. 4. The impact of the input parameters presented in Fig. 4a based on the cosine amplitude approach in Eq. (19) showed that FSC has the highest influence on the CBR_U, followed by LS, FC, PI and LL. In the case of CBR_S (Fig. 4b), FSC also has the highest influence, followed by LS, LL, FC and PI. In summary, the sensitivity analysis results indicated that FSC was the most influential input variable on CBR_U and CBR_S.

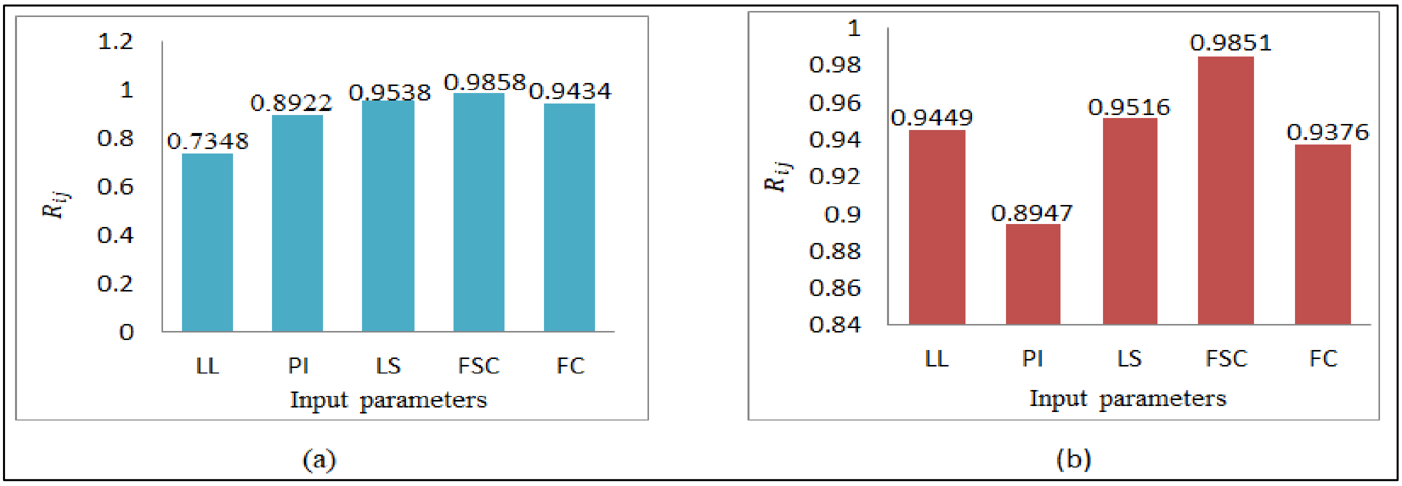

Fig 4 Strength of the input parameters on the predicted (a) CBR_U (b) CBR_S

ISSN No:-2456-2165 https://doi.org/10.38124/ijisrt/IJISRT24JUN753

V. CONCLUSIONS

The suitability of the laterite as road sub-grade, sub-base and base course depends largely on the geotechnical properties. In this study, the geotechnical assessment of eighteen selected laterite deposits in the southwest of Nigeria was carried out in the laboratory based on ASTM standard procedures to assess their appropriateness for road construction. Based on the laboratory analysis, all the laterite can be used as road subgrade while only Loc.5/S1 soil can be used as road subbase. However, none of the soil meets the specification for road base material.

The modeling of the soaked and un-soaked California bearing ratio of the soils from the index properties including liquid limit, plasticity index, linear shrinkage, fine sand content and fine content was done using ANN. The performance of the ANN models were compared with the MLR models proposed in this study and the regression based models suggested in the literature using performance indices. Based on this, ANN models outperformed all other models compared, by presenting the highest R^2 and the lowest RMSE, MAPE, and MAE values. Thus, ANN models are validated for the prediction of soaked and un-soaked California bearing ratio.

The ANN models developed were transformed into mathematical equations to enhance easy and quick prediction of laterite soaked and unsoaked California bearing ratio. The ANN mathematical models presented the same predictions as the directly ANN models. Thus, they can be used for practical purposed for determining the lateritic soils soaked and unsoaked California bearing ratio in the area.

Furthermore, sensitivity analysis conducted revealed that fine sand content (FSC) is the most influential input variable on both CBR_U and CBR_S. Thus, the FSC should not be ignored when developing model for the prediction of CBR_U and $CBR_{S,}$

- *Availability of Data*

The dataset generated during the current study are available at https://doi.org/10.6084/m9.figshare.26009728

- *Statements and Declarations*

- *Funding*

The research received no external funding.

- *Competing Interest*

The authors have no relevant financial and non-financial interests to disclose.

- *Conflict Of Interest*

The authors declare that they have no conflicts of interest.

- *Ethical Approval*

The authors state that the research was conducted according to ethical standards.

REFERENCES

[1]. **Adejumo TWE, Tsado RI 2019** Correlation of California bearing ratio with geotechnical properties of selected lateritic soils. Nigeria Institute of Civil Engineers, 17th International Conference and Annual General Meeting, 63 – 73

[2]. **Akintoriwa OJ, Ojo JS, Olorunfemi MO 2010** Geophysical investigation of pavement failure in a basement complex terrain of southwestern Nigeria. The Pacific Journal of Science and Technology, 11(2): 649 - 663

[3]. **Akan R, Keskin SN 2019** The effect of data size of ANFIS and MLR models on the prediction of unconfined compression strength of clayey soils. SN Applied Sciences, 1: 843

[4]. **Amadi AN, Akande WG, Okunlola IA, Jimoh MO, Francis DG 2015** "Assessment of the Geotechnical Properties of Lateritic Soils in Minna, North Central Nigeria for Roads Design and Construction."American Journal of Mining and Metallurgy, 3(1): 15-20. https://doi.org/10.12691/ajmm/3-1-3

[5]. **ASTM 2002** D854-02 **-** Standard test methods for specific gravity of soil by water Pycnometer. ASTM, International West Conshohocken, United State of America, 4(2): 1 – 7

[6]. **ASTM 2021** D1883-21 – Standard test methods for California bearing ratio of laboratory-compaction soil. Annual Book of ASTM Standards, West Conshohocken, PA, 19428-2959, United State of America, 4(8): 1 – 16

[7]. **ASTM 2002** D4943-02 – Standard test methods for shrinkage factors of soils by wax method. ASTM International, West Conshohocken, United States, 4(2): 1 – 5

[8]. **ASTM 2002** D422-63 – Standard test methods for particle-size analysis of soils. ASTM International, West Conshohocken, 4(8): 1 – 8

[9]. **ASTM 2021** D698-12 – Standard test methods for laboratory compaction characteristics of soil using standard effort (12,400 ft-Ibs/ft^3(600 kN-m/m)). ASTM International, West Conshohocken, Pennsylvania, United States, 4(8): 1 – 13

[10]. **ASTM 2018** D4318-17e1 – Standard test methods for liquid limit, plastic limit, plasticity index of soils. Annual book of ASTM standards, USA, 4(8): 1 – 20

[11]. **Ayodele AL, Falade FA 2016** Geotechnical properties of selected sub-base materials for road construction. Civil and Environmental Research, 8(8): 31 – 39

[12]. **Federal Ministry of Works and Housing, FMWH 1997** Nigeria General Specification for Roads and Bridges. Revised Edition 2, pp. 271

[13]. **Gudeta AD, Patel AV 2018** Prediction of CBR value from index properties of different soils: Review. International Journal of Creative Research Thoughts, 6 (2): 1190 – 1197

[14]. **Jegede G 2004** Highway pavement failure induced by poor geotechnical properties along a section of F209 Okitipupa – Igbokoda highway southwestern, Nigeria. Ife Science Journal, 6(1): 41– 44
[15]. **Jong YH, Lee CI 2004** Influence of geological conditions on the powder factor for tunnel blasting. International Journal of Rock Mechanics and Minings Sciences, 41: 533 – 538
[16]. **Khatti J, Grover KS 2021** Computation of permeability of soil using artificial intelligence approaches. International Journal of Engineering and Advance Technology, 11(1): 257 – 266
[17]. **Lawal AI 2020** An artificial neural network-based mathematical model for the prediction of blast-induced ground vibration in granite quarries in Ibadan, Oyo State Nigeria. Scientific African 8: e00413
[18]. **Lawal AI, Idris MA 2020** An artificial neural network–based mathematical model for the prediction of blast-induced ground vibrations. International Journal of Environmental Studies, 77(2): 318 – 334
[19]. **Lawal AI, Aladejare AE, Onifade M, Bada S, Idris MA 2021** Predictions of elemental composition of coal and biomass from their proximate analyses using ANFIS, ANN, and MLR. International Journal of Coal Science and Technology, 8(1): 124 – 140
[20]. **Madedor AO 1983** Pavement design guidelines and practice for diferent geological areas in Nigeria. In: Ola SA (ed) Tropical soils of Nigeria in engineering practices. Balkena Publishers, Rotterdam: 291–298
[21]. **Momoh LO, Akintoriwa O, Olorunfemi MO 2008** Geophysical Investigation of Highway failure-A Case Study from the Basement Complex Terrain of South western Nigeria. Journal of Applied Science Research, 4(6): 637 – 648
[22]. **Nwankwoala HO, Amadi AN, Ushie FA, Warmate T 2014** Determination of subsurface geotechnical properties for foundation design and construction in Akenfe community, Bayelsa State, Nigeria. American Journal of Civil Engineering and Architecture, 2 (4): 130 – 135
[23]. **Odunfa SO, Owolabi AO, Aiyedun PO, Sadiq OM 2018** Geotechnical Assessment of pavement failure along Lagos-Ibadan Expressway. FUOYE Journal of Engineering and Technology, 3(2): 113 – 117
[24]. **Ogundipe OM 2008** Road pavement failure caused by poor soil properties along Aramoko-Ilesha highway, Nigeria. Journal of Engineering and Applied Sciences, 3(3), 239-241
[25]. **Ogunribido THT, Fadairo TE 2020** Geotechnical investigation of road pavement failure along Arigidi/Oke-Agbe Akoko, Southwest, Nigeria. International Journal of Physical Research, 8(2): 35 – 39
[26]. **Onyelowe KC, Okafor FO 2013** Portland cement/quarry dust improvement of Olokoro laterite for road base. World Journal of Engineering Science India, 1(4): 133 – 143
[27]. **Owoseni JO, Adeyemi GO, Asiwaju-Bello YA, Anifowose AYB 2012** Engineering geological assessment of some lateritic soils in Ibadan, Southwestern, Nigeria using bivariate and regression analyses. Africa Journal of Science and Technology (AJST), Science and Engineering Series, 12(1): 59 – 71
[28]. **Owoyemi OO, Ajala OF, Afolagboye LO 2022** Subgrade evaluation of Gbogan-Ode Omu highway, Southwestern, Nigeria. Fuoye Journal of Pure and Applied Sciences, 7(2): 1 – 10
[29]. **Schmidhuber J 2015** “Deep learning in neural networks: An overview”. Neural Network, 61: 85-117. https://doi.org/10.1016/j.neural.2014.09.003
[30]. **Tenpe A, Kaur S 2015** Artificial neural network modeling for predicting compaction parameters based on index properties of soil. International Journal of Science and Research, 4(7): 1198 – 1201
[31]. **Tizpa P, Chenari RJ, Karimpour-Fard M, Machado SL 2014** ANN prediction of some geotechnical properties of some soil from their index parameters. Article in Arabian Journal of Geosciences, 8(5): 2911 – 2920
[32]. **Torgano ST, Ali MS, Yenealen ET, Tumato AT 2020** Correlation between CBR values and index properties of subgrade soils: in case of Bodili town. International Journal of Advance Research and Innovative Ideas in Education, 6(3): 1167 – 1182
[33]. **Werbos P 1982** Applications of advances in nonlinear sensitivity analyes. System Modeling and Optimization: 762 – 770. Retrieved 23 May 2024
[34]. **Yang Z, Yang Z 2014** Compressive biomedical physics. Karolinska institute, Stockholm, Sweden: 1. ISBN 978-0-444-53633-4. Retrieved 26 June 2023